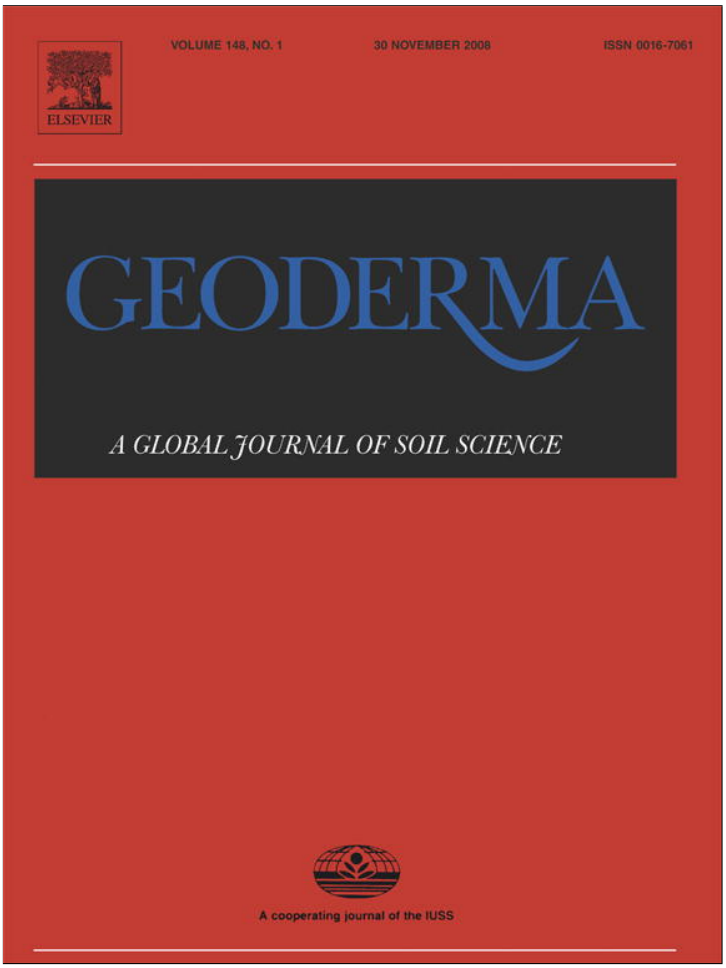

Geoderma 148 (2008) 107–112

Contents lists available at ScienceDirect

Geoderma

journal homepage: www.elsevier.com/locate/geoderma

Upgrading a 1/20,000 soil map with an apparent electrical conductivity survey

U.W.A. Vitharana [a,b,*], T. Saey [a], L. Cockx [a], D. Simpson [a], H. Vermeersch [a], M. Van Meirvenne [a]

[a] Research Group Soil Spatial Inventory Techniques, Department of Soil Management, Faculty of Bioscience Engineering, Ghent University, Coupure 653, B-9000 Gent, Belgium
[b] Department of Soil Science, Faculty of Agriculture, University of Peradeniya, Sri Lanka

ARTICLE INFO

Article history:
Received 4 April 2008
Received in revised form 17 September 2008
Accepted 18 September 2008
Available online 21 October 2008

Keywords:
Soil map upgrading
Apparent electrical conductivity
EM38
Regression kriging

ABSTRACT

Despite their shortcomings, choropleth soil maps remain the most widespread source of information on soil resources. Since most nationwide soil surveys were conducted in the second half of the previous century, a need for upgrading emerges. We evaluated the potential of detailed observations made by a mobile, non-invasive proximal soil sensor to upgrade a part of the 1/20,000 choropleth soil map of Belgium. This study was conducted on a 14 ha area which had been mapped twice in the 1950s: first, during the national soil survey yielding a 1/20,000 soil map, and second, during a detailed investigation resulting in a 1/5000 map. The first map failed to identify the presence of a Tertiary clay substratum at variable depths, while the second map indicated this substratum to be present within 1.2 m below the soil surface for about a third of the area. A recent survey with the EM38DD soil sensor provided 9192 measurements of the apparent electrical conductivity (EC_a) within the study area. The depth of the substratum (D_{ts}) was noted at 60 calibration locations by augering and the relationship between EC_a and D_{ts} was modelled by an exponential curve with an R^2 of 0.80. This allowed the detailed mapping of D_{ts} by regression kriging. The predictions were validated using 46 independent observations of D_{ts} indicating a reasonable average error of 0.24 m and a very good correlation coefficient between observed and predicted values of 0.94. A map accuracy assessment indicated that even after classification, the D_{ts} classes were better predicted by the sensor data than the 1/5000 map which was based on many more auger observations. Finally an upgraded 1/20,000 soil map was presented, illustrating the potential of combining existing soil maps with proximal soil sensing technology.

1. Introduction

Choropleth, or polygon, soil maps are the traditional source of information for land suitability analysis (Beckett and Burrough, 1971; Rossiter, 1996). During the last century, most European countries conducted nationwide surveys resulting in soil maps published on scales between 1/20,000 (e.g. Belgium) and 1/100,000 (e.g. Denmark), mostly with the aim to support agricultural development. Nowadays, increased pressure on sustainable use of limited land resources demands for land use decisions at much smaller scales (e.g. precision agriculture) and for more diverse land uses. So different decision support tools, such as process-based land evaluation frameworks, soil quality assessment and simulation models require highly detailed spatial information about soil properties (Finke, 2007). Moreover, many land characteristics vary within the recorded mapping units and ignoring this variation strongly reduces the accuracy and the reliability of choropleth soil maps (Heuvelink and Webster, 2001). Nevertheless these shortcomings, polygon-based national soil maps remain the major source of soil information available in most countries. Therefore, Finke (2007) highlighted the need to upgrade the existing polygon-based soil maps by adding new or correcting wrong information.

The traditional way to upgrade a soil map was to conduct a new survey, either at a similar scale but focussing on other soil properties, or at a more detailed scale to obtain a better representation of the spatial variability of the mapped soil properties (Dent and Young, 1981). More recently, map upgrading attempts have been made by combining the predictions obtained by interpolating soil observations with predictions by soil polygon maps (Voltz and Webster, 1990; Van Meirvenne et al., 1994). But these invasive methods require large field survey efforts and thus they are often limited by the cost and time constraints associated with intensive field sampling and laboratory analysis (Oberthür et al., 1999). Recent developments in proximal non-invasive soil sensing techniques offer new opportunities to improve the soil map accuracy with considerable reductions in sampling effort (Adamchuk et al., 2004).

Our objective was to compare a more detailed soil map (scale 1/5000) with mobile measurements of the apparent electrical conductivity obtained with a georeferenced electromagnetic induction

* Corresponding author. Research Group Soil Spatial Inventory Techniques, Department of Soil Management, Faculty of Bioscience Engineering, Ghent University, Coupure 653, B-9000 Gent, Belgium. Tel.: +32 9 264 5869.
E-mail address: u.vitharana@live.com (U.W.A. Vitharana).

0016-7061/$ – see front matter © 2008 Elsevier B.V. All rights reserved.
doi:10.1016/j.geoderma.2008.09.013

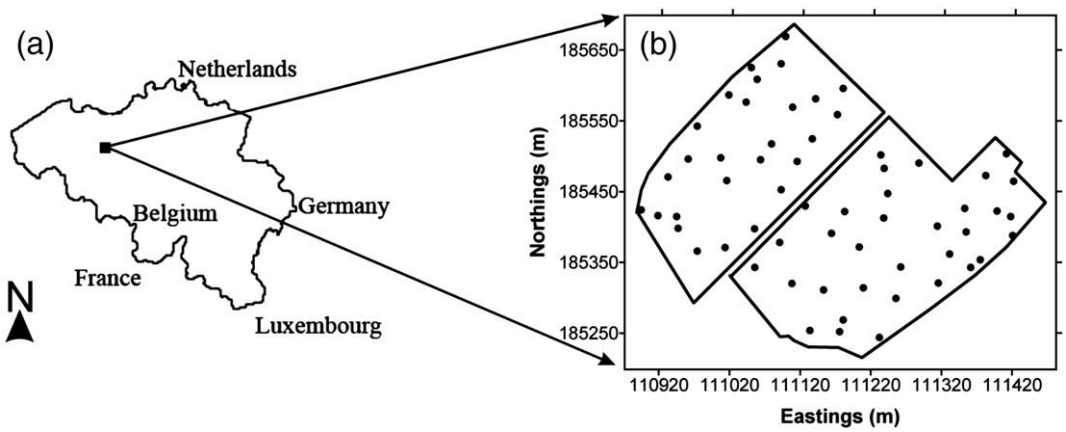

Fig. 1. (a) Localization of the study area in Belgium and (b) study area with observation points of the depth to the Tertiary clay substratum.

(EMI) soil sensor (the EM38DD) to upgrade an existing 1/20,000 soil map. This objective will be evaluated for a 14 ha area in Belgium, where the existing soil map needs to be upgraded with information on the depth to a Tertiary substratum.

2. Materials and methods

2.1. Study area

The 14 ha study area was located in Melle, Belgium, with central coordinates: 50° 58′ 42″ N and 3° 49′ 00″ E (Fig. 1). This area is a part of the Ghent University agricultural research farm and situated in the sandy silt (sandy loam to silt loam in the USDA textural classification) agro-pedological region of the country. During the Weichselian glacial stage of the Late Pleistocene (80 ka–10 ka), wind-blown loess was deposited over this area, covering the surfacing Tertiary layers. This loess cover can have a substantial thickness in the depressions (5–10 m), but it can diminish to some tens of centimetres on the ridges. The Tertiary substratum consists of sandy or clayey formations from the Early Eocene (55 Ma–49 Ma). The elevation of the study area declines gradually from 22 m above mean sea level in the western corner to 15 m in the eastern corner.

2.2. 1/20,000 soil map

The Belgian national soil survey was conducted between 1947 and 1973. It proceeded by taking soil auger observations, down to 1.25 m, at an average density of one observation per 0.7 to 1 ha. Within the study area this map indicated the presence of two soil series (see further Fig. 6b). Approximately two-third of the area belongs to series 'Ldc', which represents a sandy silt topsoil texture ('L') (according to Belgian soil textural triangle; Tavernier and Maréchal, 1962), moderately wet conditions (drainage class 'd') with a strongly degraded textural B-horizon (profile development type 'c'). The remaining part of the study area is characterized by the soil series 'Lcc', with a similar topsoil texture and profile development but with drier moisture conditions (drainage class 'c'). These soil types correspond to Albeluvisols according to the WRB classification system (FAO/ISRIC/ISSS, 1998). The Belgian soil map legend used a prefix to indicate the depth and nature of a shallow substratum observable within augering depth (a substratum represents a contrasting layer with a different texture). If a clayey substratum was encountered in the top 0.75 m, a prefix 'u' was added to the soil series. When this substratum was found between 0.75 and 1.25 m then the prefix was '(u)'. No prefix implicated that no substratum was observed within 1.25 m from the soil surface. The latter situation is the case in our study area, where according to the soil map there should be no substratum within the top 1.25 m (Fig. 2(a)).

2.3. 1/5000 soil map

Since our study area is a part of the experimental farm of the UGent, it was surveyed again in more detail in 1951. Therefore, an intensive survey was conducted with about 15 observations per ha, summing to approximately 210 augerings within the study area. This resulted in a choropleth soil map at a scale of 1/5000. For unclear reasons, the depth limits were slightly modified: 0.6 and 1.2 m instead

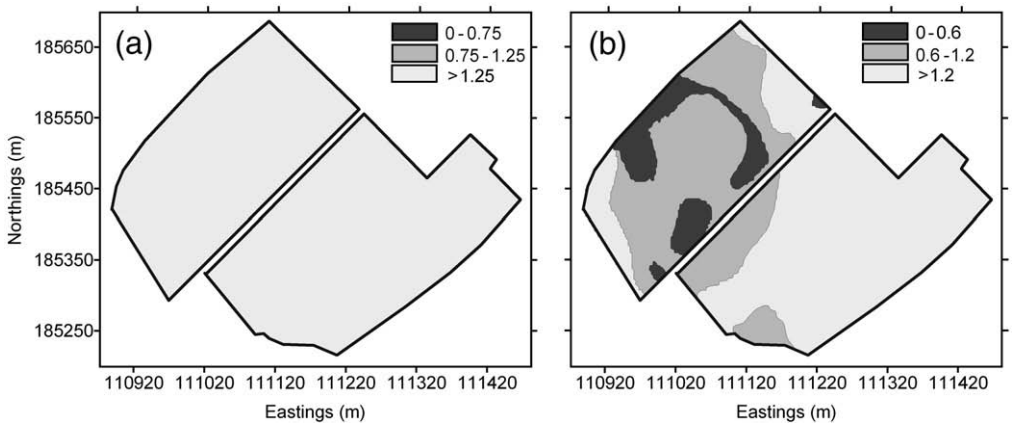

Fig. 2. Information about the depth to the clay substratum (D_{ts}) as provided by the two soil maps: (a) at a scale of 1/20,000 and (b) at a scale of 1/5000.

Table 1
Descriptive statistics of EC_a measured in horizontal (EC_a−H) and vertical (EC_a−V) dipole modes (9192 samples) and of the 60 observations of the depth to the Tertiary clay substratum (D_{ts})

	Mean	Minimum	Maximum	SD[a]	CV[b]	Skewness
EC_a−V (mS m^{-1})	47.2	22.2	78.0	11.9	25.3	0.07
EC_a−H (mS m^{-1})	38.9	20.8	64.4	7.7	19.8	0.15
D_{ts} (m)	1.6	0.5	2.9	0.65	41.1	0.18

[a] SD = standard deviation.
[b] CV = coefficient of variation (%).

of 0.75 and 1.25 m as used on the 1/20,000 map. Contrarily to the 1/20,000 map, this map indicated the presence of a clayey substrate within 1.2 m, in some parts even within 0.6 m, over about a third of the area (Fig. 2(b)).

2.4. EMI soil sensor

We applied EMI to measure the apparent electrical conductivity (EC_a in mS m^{-1}) of our study area. Therefore the dual dipole EM38DD (Geonics Limited, ON, Canada) soil sensor was used. This sensor operates simultaneously in horizontal and vertical dipole orientations providing EC_a−H and EC_a−V measurements, respectively. Seventy percent of the response of these signals comes from the top 0.75 m, and top 1.60 m, of the soil, respectively (McNeil, 1980). In April 2006, the sensor was mounted on a sled which was pulled by an all terrain vehicle at a speed of about 15 km h^{-1} along 4 m spaced parallel-lines guided by a light-bar guidance system. Every second, EC_a−H and EC_a−V measurements were recorded by a field computer together with an Omnistar corrected Trimble AgGPS332 (Trimble Navigation Limited, CA, USA) signal to georeference the measurements accurately. To calibrate the EC_a measurements, 60 observations were made of the depth to the Tertiary clay substratum (D_{ts}). Fifty-five locations were selected using a stratified random procedure picking randomly one location within cells of 50 by 50 m. The remaining five observations were located along the edges of the study area (Fig. 1(b)). At all locations a distinct and abrupt boundary was observed between the Pleistocene sediment and the underlying Tertiary clay substratum within a depth of 3 m. Sometimes pebbles indicated the presence of a former erosion surface on top of the Tertiary layer facilitating its identification.

2.5. Data analysis

D_{ts} was interpolated using regression kriging (Odeh et al., 1995). Therefore, the D_{ts} estimate at any unsampled location ($z^*(\mathbf{x}_0)$) was obtained in five steps: (1) EC_a−V was interpolated to a 2.5 m×2.5 m grid by ordinary kriging procedure with local variograms (Minasny et al., 2005; Taylor et al., 2007); (2) a regression analysis was used to fit a model describing the relationship between EC_a−V and D_{ts}, then the latter was predicted at every grid location $\mathbf{x}_0$, yielding $D_{ts,r}{}^*(\mathbf{x}_0)$; (3) at the 60 locations where D_{ts} was measured, $\mathbf{x}_\alpha$ (α=1,…, 60), the difference between the observed and predicted depth was calculated as:

$$r(\mathbf{x}_\alpha) = \left\{ D_{ts}(\mathbf{x}_\alpha) - D_{ts,r}{}^*(\mathbf{x}_\alpha) \right\}$$

resulting in 60 residuals $r(\mathbf{x}_\alpha)$; (4) these residuals were interpolated to every grid node $\mathbf{x}_0$ using simple kriging with a mean of zero and the variogram of the residuals $\hat{\gamma}(\mathbf{h})$:

$$\hat{\gamma}(\mathbf{h}) = \frac{1}{2N(\mathbf{h})} \sum_{\alpha=1}^{N(\mathbf{h})} \{ r(\mathbf{x}_\alpha + \mathbf{h}) - r(\mathbf{x}_\alpha) \}^2$$

with $N(\mathbf{h})$ the number of pairs of residuals $\{r(\mathbf{x}_\alpha), r(\mathbf{x}_\alpha+\mathbf{h})\}$ separated by a distance vector $\mathbf{h}$; (5) $D_{ts,r}{}^*(\mathbf{x}_0)$ and the interpolated residuals $r(\mathbf{x}_0)^*$ were added to obtain the prediction of $D_{ts}{}^*$ at every grid node:

$$D_{ts}{}^*(\mathbf{x}_0) = D_{ts,r}{}^*(\mathbf{x}_0) + r(\mathbf{x}_0)^*.$$

The accuracy of the D_{ts} predictions was validated by 46 additional observations of D_{ts}. These observations were taken along three transects ensuring that both the smallest and largest D_{ts} predicted by EMI sensing and 1/5000 map were visited adequately. The prediction accuracy was evaluated by calculating three validation indices: the mean prediction error (MPE), the root mean squared prediction error (RMSPE) and the Pearson correlation coefficient (r) between the predictions and the measurements.

To evaluate the accuracies of the different soil maps, class predictions by each map were compared with 46 ground truth observations. The result was summarised in a confusion matrix (Lillesand and Kiefer, 1994). Every element of this matrix (x_{lk}) represents the number of ground truth observations belonging to the depth class k which belongs to class l of the soil map. The diagonal elements (x_{kk}) represent the agreement between the observations and map predictions. The overall map accuracy (θ_1) was calculated as:

$$\theta_1 = \frac{1}{n} \sum_{k=1}^{K} x_{kk}$$

with n the total number of validation observations and K the number of classes. However, not all favourable θ_1 values implicate high map accuracies, because some classes may occupy much larger areas than others and thus dominate the validation sample (Finke, 2007). Therefore, the interpretation of θ_1 needs to be supplemented with a kappa index of overall agreement (κ) obtained from (Cohen, 1960):

$$\kappa = \frac{\theta_1 - \theta_2}{1 - \theta_2}$$

given that $\theta_2 = \frac{1}{n^2} \sum_{k=1}^{K} x_{k.} x_{.k}$ with $x_{k.}$ and $x_{.k}$ the marginal sums of rows and columns of the confusion matrix. This index provides an indication of the non-coincidental agreement between the observations and the predictions and ranges from −1 to 1. Landis and Koch

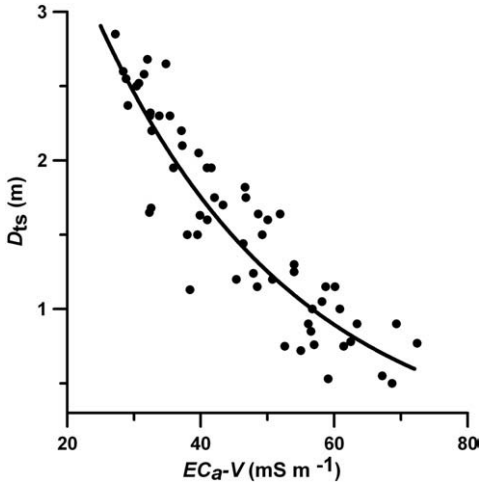

Fig. 3. Depth to the Tertiary clay substratum (D_{ts}) as a function of apparent electrical conductivity measured with the EM38DD in the vertical dipole mode (EC_a−V) with empirical exponential regression fit.

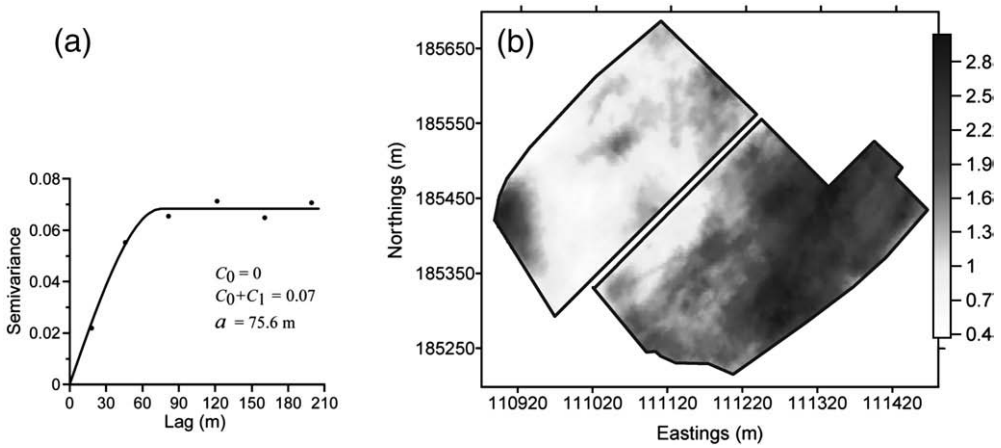

Fig. 4. (a) Theoretical (curve) semivariogram model (with fitted parameters) fitted to the experimental semivariogram (points) for the depth to the Tertiary clay substratum (D_{ts}) residuals and (b) map of interpolated D_{ts} predictions obtained after regression kriging.

(1977) divided this range into classes with the aim of providing an indication about the degree of correspondence: ≤0=poor, 0.01–0.20=slight, 0.21–0.40=fair, 0.41–0.60=moderate, 0.61–0.80=substantial and 0.81–1=almost perfect.

3. Results and discussion

3.1. Relationship between EC_a and D_{ts}

On average, the 9192 EC_a–V measurements were larger than the colocated EC_a–H measurements (Table 1), which indicated the presence of a higher conductive subsoil below less conductive topsoil. The coefficient of variations of the two distributions indicated a larger variation of EC_a–V. However, both measurements showed an approximate symmetric distribution, as shown by their near to zero coefficient of skewness. Moreover, a very strong correlation between both measurements (r=0.98) and identical spatial patterns indicated the large degree of similarity of both measurements.

The D_{ts} observations revealed its presence at shallow to deeper depths (Table 1) across the study area. Nevertheless, a large variation of observations was evident by its coefficient of variation value. The small skewness coefficient proved that the distribution of D_{ts} is almost symmetrical. According to the class limits used for the 1/20,000 soil map legend, 12% of the observations was classified as shallow (≤0.75 m), 28% as moderate (>0.75 m and ≤1.25 m) and 60% as deep (>1.25 m).

The correlations between D_{ts} and EC_a–V and D_{ts} and EC_a–H were negative: −0.90 and −0.87, respectively. Considering the higher correlation and deeper sensing depth we preferred the EC_a–V measurements as a covariate to predict D_{ts}. The relationship between these two variables was best fit by an exponential regression (Fig. 3) with a coefficient of determination (R^2) of 0.80:

$$D_{ts} = 6.7 \exp(-0.03\, EC_a\text{–V}).$$

Similar strong non-linear relationships between interface depths of contrasting soil layers and EC_a were observed by Doolittle et al. (1994), Cockx et al. (2007) and Saey et al. (2008). However, Brus et al. (1992) reported a poor non-linear relationship between EC_a and depth to boulder clay substratum, probably due to a lack of sufficiently strong contrast in textural composition between the boulder clay and the material above it.

3.2. Mapping D_{ts}

An isotropic spherical variogram was found to represent the experimental variogram of the residuals best (Fig. 4a):

$$\gamma(h) = C_0 + C_1\left\{\frac{3h}{2a} - \frac{1}{2}\left(\frac{h}{a}\right)^3\right\} \quad \text{if} \quad 0 < h \le a$$
$$\gamma(h) = C_0 + C_1 \quad \text{if} \quad h > a, \text{ and}$$
$$\gamma(0) = 0$$

The map of D_{ts}* is given in Fig. 4b. It can be observed that the Tertiary clay substratum was predicted to occur quite deep (1.5–2.7 m) in the western corner of the study area, which coincides with the highest soil surface elevations within the study area. Shallow to moderate depths (0.4–1.50 m) were mapped over the largest part of the western half of the study area. This undeep position of the substratum can be expected to influence crop performance and soil management, hence the importance to map it accurately. In the eastern part, the substratum was predicted to occur deeper again (1.5–3.0 m).

3.3. Validation of D_{ts} predictions

The MPE was 0.02 m, the RMSPE was 0.24 m and r was 0.94 (Fig. 5). The combination of the near-to zero MPE value and a close to one r

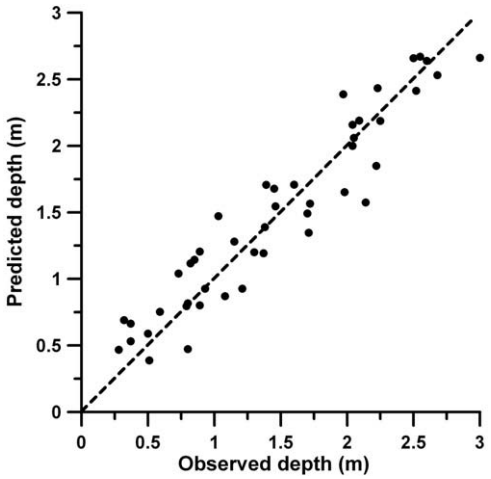

Fig. 5. Validation of predicted depth to the Tertiary clay substratum (D_{ts}) using 46 observed depths.

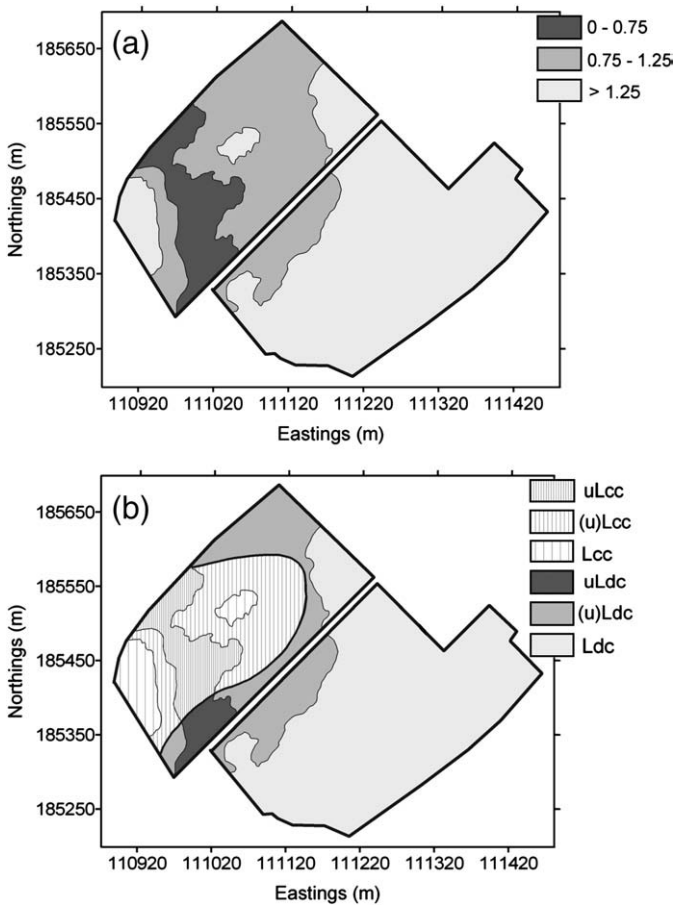

Fig. 6. (a) Predicted depth to the Tertiary clay substratum (D_{ts}) classified according to the legend of the 1/20,000 Belgian national soil map and (b) the upgraded 1/20,000 soil map. The inner thick boundary separates the two soil series Lcc and Ldc.

value indicated that the predictions were on average aligned close to the 1–1 line of the scatter plot. An average prediction error of 0.24 m is quite acceptable given the range of this variable and the measurement errors associated with auger observations in the field.

To quantify and compare the different map accuracies, both θ_1 and κ were calculated for the two soil maps (Fig. 2(a) and (b)) and the map of D_{ts} predictions (Fig. 4(b)) classified according to the depth class limits of the 1/20,000 map. The 1/20,000 soil map, which did not indicate any variation in D_{ts}, had a $\theta_1 = 0.60$ with a $\kappa = 0$. Obviously these values indicate a poor map accuracy in respect to the prediction of D_{ts}. The 1/5000 soil map had a larger overall accuracy ($\theta_1 = 0.83$) and kappa index ($\kappa = 0.70$) which represent a much better correspondence between observed and predicted depth classes. The classified D_{ts} map obtained with the EMI sensor (Fig. 6a) was found to be the most accurate, with $\theta_1 = 0.89$ and an excellent $\kappa = 0.82$.

3.4. Upgrading the 1/20,000 soil map

The upgrading of the 1/20,000 choropleth soil map can be done either by incorporating the predicted D_{ts} information as a continuous layer into the 1/20,000 digitized soil map or by redefining soil series based on this new information. Here we implemented the second approach to facilitate a comparison with the two choropleth maps. Therefore, the D_{ts} predictions classified according to the 1/20,000 map legend, were added to the soil map. A few very small map units (<0.1 ha) were omitted. The resulting upgraded 1/20,000 soil map is given in Fig. 6b.

The upgraded 1/20,000 soil map divides the two original two soil series into six variants. The western half of the study area was strongly modified compared to the original map. Unlike the original map, nearly half of the upgraded map is covered with soil series denoting the presence of a shallow (prefix 'u') or a moderately deep (prefix '(u)') Tertiary clay substratum. The classification of the predicted D_{ts} map into substratum classes according to the conventional legend did not include D_{ts} classes below the lower limit of 1.25 m. Therefore, no modifications took place in the eastern part of the study area.

4. Conclusions

In our study area, the national soil survey produced a 1/20,000 soil map based on approximately 14–20 soil augerings. These failed to identify the presence of a Tertiary clay substratum within 1.25 m below the soil surface. A more detailed survey, based on approximately 210 augerings, allowed to produce a 1/5000 map that indicated the presence of a substratum at various depths. An accuracy assessment of this map revealed that it predicted D_{ts} much better ($\theta_1 = 0.83$ and $\kappa = 0.70$) than the original 1/20,000 map. So this indicates that the past solution to improve detailed map predictions by increasing the map scale and taking more observations proved to be successful.

Modern technology, however, allows to go a step further. More than nine thousand EC_a observations obtained with the EM38DD sensor provided abundant information which could be strongly linked to the depth of the Tertiary substratum. We used 60 augerings to establish this relationship. Predictions were validated and found to be sufficiently accurate. After classifying these predictions the accuracy of the map was superior to the 1/5000 map: $\theta_1 = 0.89$ and a $\kappa = 0.82$. This study demonstrates the potential of EMI-based proximal soil sensors to upgrade existing soil maps.

Acknowledgements

Udayakantha W.A. Vitharana thanks the Ghent University for providing financial support under the special research fund (BOF) to carry out this study. The authors thank the UGent agricultural research farm (Biocentrum Agri-Vet) for granting access to their fields and Prof. Roger Langohr for helpful explanations on 1/5000 soil map.

References

Adamchuk, V.I., Hummel, J.W., Morgan, M.T., Upadhyaya, S.K., 2004. On-the-go soil sensors for precision agriculture. Computers and Electronics in Agriculture 44, 71–91.
Beckett, P.H.T., Burrough, P.A., 1971. Relation between cost and utility in soil survey IV. Comparison of utilities of soil maps produced by different survey procedures, and to different scales. Journal of Soil Science 22, 466–480.
Brus, D.J., Knotters, M., Van Dooremolen, W.A., Van Kernebeek, P., Van Seeters, R.J.M., 1992. The use of electromagnetic measurements of apparent soil electrical conductivity to predict the boulder clay depth. Geoderma 55, 79–93.
Cockx, L., Van Meirvenne, M., De Vos, B., 2007. Using the EM38DD soil sensor to delineate clay lenses in a sandy forest soil. Soil Science Society of America Journal 71, 1314–1322.
Cohen, J., 1960. A coefficient of agreement for nominal scales. Educational and Psychological Measurement 20, 37–46.
Dent, D., Young, A., 1981. Soil Survey and Land Evaluation. George Allen & Unwin Ltd, London, UK.
Doolittle, J.A., Sudduth, K.A., Kitchen, N.R., Indorante, S.J., 1994. Estimating depths to claypans using electromagnetic induction methods. Journal of Soil and Water Conservation 49, 572–575.
FAO/ISRIC/ISSS, 1998. World reference base for soil resources. World soil resources report. FAO, Rome.
Finke, P.A., 2007. Quality assessment of digital soil maps: producers and users perspective. In: Lagacherie, P., McBratney, A.B., Voltz, M. (Eds.), Digital Soil Mapping: An Introductory Perspective. Elsevier, Amsterdam, pp. 523–541.
Heuvelink, G.B.M., Webster, R., 2001. Modelling soil variation: past, present, and future. Geoderma 100, 269–301.
Landis, J.R., Koch, G.G., 1977. Measurement of observer agreement for categorical data. Biometrics 33, 159–174.
Lillesand, T.M., Kiefer, R.W., 1994. Remote Sensing and Image Interpretation. John Wiley & Sons, NY.
Minasny, B., McBratney, A.B., Whelan, B.M., 2005. VESPER version 1.62. Australian Centre for Precision Agriculture, McMillan Building A05, The University of Sydney, NSW 2006.
McNeil, J.D., 1980. Electromagnetic Terrain Conductivity Measurement at Low Induction Numbers: Technical Note TN-6. GEONICS Limited, Ontario.

Oberthür, T., Goovaerts, P., Dobermann, A., 1999. Mapping soil texture classes using field texturing, particle size distribution and local knowledge by both conventional and geostatistical methods. European Journal of Soil Science 50, 457–479.

Odeh, I.O.A., McBratney, A.B., Chittleborough, D.J., 1995. Further results on prediction of soil properties from terrain attributes — heterotopic cokriging and regression-kriging. Geoderma 67, 215–226.

Rossiter, D.G., 1996. A theoretical framework for land evaluation. Geoderma 72, 165–190.

Saey, T., Simpson, D., Vitharana, U.W.A., Vermang, J., Van Meirvenne, M., 2008. Reconstructing the paleotopography beneath the loess cover with the aid of an electromagnetic induction sensor. Catena 74, 58–64.

Taylor, J.A., McBratney, A.B., Whelan, B.M., 2007. Establishing management classes for broadacre agricultural production. Agronomy Journal 99, 1366–1376.

Tavernier, R., Maréchal, R., 1962. Soil and soil classification in Belgium. In: Neale, G.J. (Ed.), Transactions of Joint Meeting of Commissions IV and V. International Society of Soil Science, Soil Bureau, P.B. Lower Hutt, New Zealand, pp. 298–307.

Van Meirvenne, M., Scheldeman, K., Baert, G., Hofman, G., 1994. Quantification of soil textural fractions of Bas-Zaire using soil map polygons and or point observations. Geoderma 62, 69–82.

Voltz, M., Webster, R., 1990. A comparison of kriging, cubic-splines and classification for predicting soil properties from sample information. Journal of Soil Science 41, 473–490.